

Fingerprint Enhancement Using STFT Analysis

Sharat Chikkerur * Alexander N. Cartwright Venu Govindaraju

Center for Unified Biometrics and Sensors, University at Buffalo, NY, USA

Abstract

Contrary to popular belief, despite decades of research in fingerprints, reliable fingerprint recognition is still an open problem. Extracting features out of poor quality prints is the most challenging problem faced in this area. This paper introduces a new approach for fingerprint enhancement based on Short Time Fourier Transform(STFT) Analysis. STFT is a well known technique in signal processing to analyze non-stationary signals. Here we extend its application to 2D fingerprint images. The algorithm simultaneously estimates all the intrinsic properties of the fingerprints such as the foreground region mask, local ridge orientation and local ridge frequency. Furthermore we propose a probabilistic approach of robustly estimating these parameters. We experimentally compare the proposed approach to other filtering approaches in literature and show that our technique performs favorably.

Key words: fingerprint image enhancement, STFT analysis, filtering

PACS: 1.000, 1.001, 7.002, 7.008

1 Introduction

The performance of a fingerprint feature extraction and matching algorithm depends critically upon the quality of the input fingerprint image. While the 'quality' of a fingerprint image cannot be objectively measured, it roughly corresponds to the clarity of the ridge structure in the fingerprint image. Where as a 'good' quality fingerprint image has high contrast and well defined ridges and valleys, a 'poor' quality fingerprint is marked by low contrast and ill-defined boundaries between the ridges. There are several reasons that may degrade the quality of a fingerprint image.

- (1) Presence of creases, bruises or wounds may cause ridge discontinuities.
- (2) Excessively dry fingers lead to fragmented and low contrast ridges.
- (3) Sweat on fingerprints leads to smudge marks and connects parallel ridges.

* The author can be reached at ssc5@cubs.buffalo.edu



Fig. 1. Fingerprint images of different quality. The quality decreases from left to right. (a) Good quality image with high contrast between the ridges and valleys (b) Insufficient distinction between ridges and valleys in the center of the image (c,d) Dry prints

The quality of fingerprint encountered during verification varies over a wide range as shown in Figure 1. It is estimated that roughly 10% of the fingerprint encountered during verification can be classified as 'poor' [1]. Poor quality fingerprints lead to generation of spurious minutiae. In smudgy regions, genuine minutiae may also be lost, the net effect of both leading to loss in accuracy of the matcher.

The robustness of the recognition system can be improved by incorporating an enhancement stage prior to feature extraction. Due to the non-stationary nature of the fingerprint image, general-purpose image processing algorithms are not very useful in this regard but serve only as a preprocessing step in the overall enhancement scheme. Furthermore, pixel oriented enhancement schemes like histogram equalization [2], mean and variance normalization [3], Wiener filtering [4] improve the legibility of the fingerprint but do not alter the ridge structure. Also, the definition of noise in a generic image and a fingerprint are widely different. The *noise* in a fingerprint image consists of breaks in the directional flow of ridges. In the next section, we will discuss some previous filtering approaches that were designed to enhance the ridge structure specifically.

2 Prior Related Work

Due to the non-stationary nature of the fingerprint image, a single filter that operates on the entire image is not practical. Instead, the filter parameters should be adapted to enhance the local ridge structure. Consequently, a majority of the existing techniques are based on the use of *contextual* filters whose parameters depend on the local ridge frequency and orientation. The context information includes

- (1) *Ridge continuity*: The underlying morphogenetic process that produced the ridges does not allow for irregular breaks in the ridges except at ridge endings.

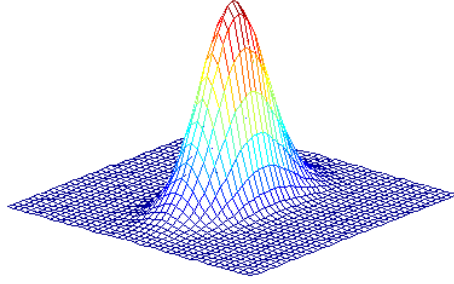


Fig. 2. The anisotropic filtering kernel proposed by Greenberg et. al [4]. The filter shown has $S=-2$, $V=10$, $\sigma_1^2(x_0) = 4$ $\sigma_2^2(x_0) = 2$

-
- (2) *Regularity*: Although the fingerprint represents a non-stationary image, the intrinsic properties such as instantaneous orientation and ridge frequency varies slowly across the fingerprint surface.

Due to the regularity and continuity properties of the fingerprint image occluded and corrupted regions can be recovered using the contextual information from the surrounding neighborhood. Hong et al. [3] label such regions as '*recoverable*' regions. The efficiency of an automated enhancement algorithm depends on the extent to which they utilize contextual information. The filters themselves may be defined in spatial or in the Fourier domain.

2.1 Spatial Domain Filtering

O’Gorman et al. [5] proposed the use of contextual filters for fingerprint image enhancement for the first time. They use an anisotropic smoothing kernel whose major axis is oriented parallel to the ridges. For efficiency, they precompute the filter in 16 directions. The filter increases contrast in a direction perpendicular to the ridges while performing smoothing in the direction of the ridges. Recently, Greenberg et al. [4] proposed the use of an anisotropic filter that is based on structure adaptive filtering by Yang et al. [6]. The filter kernel is adapted at each point in the image and is given by

$$f(x, x_0) = S + V\rho(x - x_0)\exp\left\{-\left(\frac{((x - x_0).n)^2}{\sigma_1^2(x_0)} + \frac{((x - x_0).n_\perp)^2}{\sigma_2^2(x_0)}\right)\right\} \quad (1)$$

Here n and n_\perp represents unit vectors parallel and perpendicular to the ridges respectively. σ_1 and σ_2 control the eccentricity of the filter. $\rho(x - x_0)$ determines the support of the filter and chosen such that $\rho(x) = 0$ when $|x - x_0| > r$.

Another approach based on directional filtering kernel is by Hong et al. [3]. The main stages of their algorithm are as follows

- (1) *Normalization*: This procedure normalizes the global statistics of the image, by reducing each image to a fixed mean and variance. Although this pixel wise operation does not change the ridge structure, the contrast and brightness of the image are normalized as a result. The normalized image is defined as

$$G(i, j) = \begin{cases} M_0 + \sqrt{\frac{VAR_0((I-M)^2)}{VAR}}, & \text{if } I(i, j) > M \\ M_0 - \sqrt{\frac{VAR_0((I-M)^2)}{VAR}}, & \text{otherwise} \end{cases} \quad (2)$$

- (2) *Orientation Estimation*: This step determines the dominant direction of the ridges in different parts of the fingerprint image . This is a critical process and errors occurring at this stage are propagated into the frequency estimation and filtering stages. More details are discussed w.r.t intrinsic images (see section 2.3)
- (3) *Frequency Estimation*: This step is used to estimate the inter-ridge separation in different regions of the fingerprint image. More techniques for frequency estimation are discussed w.r.t intrinsic images (see section 2.3)
- (4) *Segmentation*: In this step, a region mask is derived that distinguishes between 'recoverable' and 'unrecoverable' portions of the fingerprint image.
- (5) *Filtering*: Finally, using the context information consisting of the dominant ridge orientation and ridge separation, a band pass filter is used to enhance the ridge structure.

The algorithm uses a properly oriented Gabor kernel for performing the enhancement. Gabor filters have important signal properties such as optimal joint space frequency resolution [7]. Gabor elementary functions form a very intuitive representation of fingerprint images since they capture the periodic, yet non-stationary nature of the fingerprint regions. Daugman [8] and Lee [9] have used Gabor elementary functions to represent generic 2D images. The even symmetric form of the Gabor elementary function that is oriented at an angle 0° is given by

$$G(x, y) = exp \left\{ -\frac{1}{2} \left[\frac{x^2}{\delta_x^2} + \frac{y^2}{\delta_y^2} \right] \right\} cos(2\pi f x) \quad (3)$$

Here f represents the ridge frequency and the choice of δ_x^2 and δ_y^2 determines the shape of the filter envelope and also the trade of between enhancement and spurious artifacts. If $\delta_x^2 \geq \delta_y^2$ results in excessive smoothing in the direction of the ridges causing discontinuities and artifacts at the boundaries. The filter for any other direction ϕ may be obtained by rotating the elementary kernel. The determination of the ridge orientation and ridge frequencies are discussed in detail in section 2.3. This is by far, the most popular approach for fingerprint enhancement. While the compact support of the Gabor kernel is beneficial from a time-frequency analysis perspective, it does not necessarily translate to an efficient means for enhancement. Our algorithm is based on a filter that has separable radial and angular components and is tuned specifically to the distribution of orientation and frequencies in the

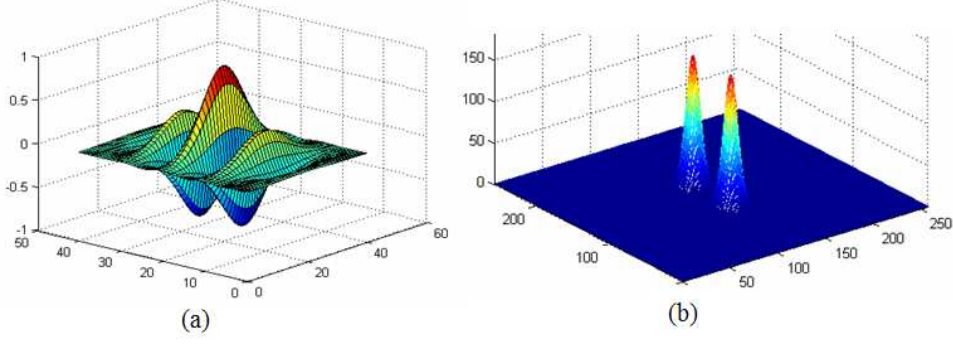


Fig. 3. (a)Real part of the gabor (b) The Fourier spectrum of the Gabor kernel showing the localization in the frequency domain

local region of the fingerprint image. Other approaches based on spatial domain techniques can be found in [10]. More recent work based on reaction diffusion techniques can be found in [11,12]

2.2 Fourier Domain Filtering

This section deals with filters that are defined explicitly in the Fourier domain. This excludes discussion of spatial convolution methods that are accomplished in the Fourier domain. Sherlock and Monroe [13] perform contextual filtering completely in the Fourier domain. Each image is convolved with precomputed filters of the same size as the image. The precomputed filter bank (labeled $PF_0, PF_1 \dots PF_N$ in Figure 4) are oriented in eight different direction in intervals of 22.5° . However, the algorithm assumes that the ridge frequency is constant through out the image in order to prevent having a large number of precomputed filters. Therefore the algorithm does not utilize the full contextual information provided by the fingerprint image. The filter used is separable in radial and angular domain and is given by

$$H(\rho, \phi) = H_\rho(\rho)H_\phi(\phi) \quad (4)$$

$$H_\rho(\rho) = \sqrt{\left[\frac{(\rho\rho_{BW})^{2n}}{(\rho\rho_{BW})^{2n} + (\rho^2 - \rho_0^2)^{2n}} \right]} \quad (5)$$

$$H_\phi(\phi) = \begin{cases} \cos^2 \frac{\pi}{2} \frac{(\phi - \phi_c)}{\phi_{BW}} & \text{if } |\phi| < \phi_{BW} \\ 0 & \text{otherwise} \end{cases} \quad (6)$$

Here $H_\rho(\rho)$ is a band-pass butterworth filter with center defined by ρ_0 and bandwidth ρ_{BW} . The angular filter is a raised cosine filter in the angular domain with support ϕ_{BW} and center ϕ_c . However, the precomputed filters mentioned before are location independent. The contextual filtering is actually accomplished at the stage

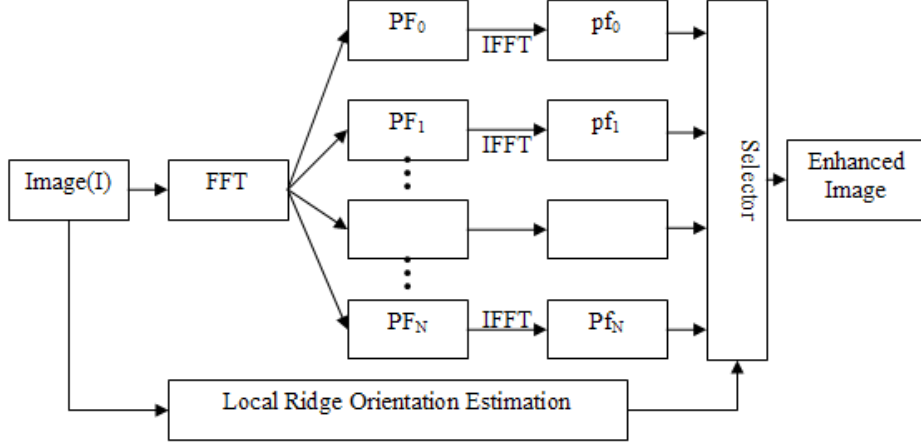


Fig. 4. Block diagram of the filtering scheme proposed by Sherlock and Monro [13]

labeled 'selector'. The 'selector' uses the local orientation information to combine the results of the filter bank using appropriate weights for each output. The algorithm also accounts for the curvature of the ridges, something that was overlooked by the previous filtering approaches including Gabor filtering. In regions of high curvature, the assumption of a single dominant ridge direction is not valid. Having a fixed angular bandwidth lead to spurious artifacts and subsequently spurious minutiae. In the approach proposed by Sherlock et al. the angular bandwidth of the filter is taken as a piece wise linear function of the distance from the singular points such as core and delta. However, this requires that the singular point be estimated accurately, a difficult task in poor quality images. In our algorithm, we utilize the angular coherence measure proposed by Rao [14]. This is more robust to errors in the orientation estimation and does not require us to compute the singular point locations. The results in their paper also indicate that while the algorithm is able to eliminate most of the false minutiae, it also misses more number of genuine minutiae when compared to other existing algorithms.

Watson et al. [15] proposed another approach for performing enhancement completely in the Fourier domain. This is based on 'root filtering' technique [16]. In this approach the image is divided into overlapping block and in each block, the enhanced image is obtained by

$$I_{enh}(x, y) = FFT^{-1}\{F(u, v)|F(u, v)|^k\} \quad (7)$$

$$F(u, v) = FFT(I(x, y)) \quad (8)$$

Another advantage of this approach is that it does not require the computation of intrinsic images (Section 2.3) for its operation. This has the effect of increasing the dominant spectral components while attenuating the weak components. This resembles matched filtering very closely. However, in order to preserve the phase, the enhancement also retains the original spectrum $F(u, v)$.

2.3 *Intrinsic Images*

The *intrinsic images* represent the important properties of the fingerprint image as a pixel map. These include

- (1) **Orientation Image:** The orientation image \mathbf{O} represents the instantaneous ridge orientation at every point in the fingerprint image. However, in practice the orientation image is computed at a much lower resolution (assigning an orientation for each block of the image). The ridge orientation is not defined in regions where the ridges are not present.
- (2) **Frequency Image:** The local ridge frequency indicates the average inter ridge distance within a block. Similar to the orientation image, the ridge frequency is not defined for the background regions.
- (3) **Region Mask:** The region mask indicates the parts of the image where ridge structures are present. It is also known as the foreground mask. Some techniques [3] are even able to distinguish between recoverable and unrecoverable regions.

The computation of the intrinsic images forms a very critical step in the feature extraction process. Errors in computing these propagate through all the stages of the algorithm. In particular, errors in estimation of ridge orientation will affect enhancement, feature extraction and as a consequence the accuracy of the recognition. Applications that require a reliable orientation map include enhancement [3,13,5,17], singular point detection [18–20] and segmentation [21] and most importantly fingerprint classification. The region mask is used to eliminate spurious minutiae [17,3].

2.3.1 *Orientation Image*

There have been several approaches to estimate the orientation image of a fingerprint image. These include the use of gradients [3], filter banks [22], template comparison [20], and ridge projection based methods [13]. The orientation estimation obtained by these methods is noisy and have to be smoothed before further use. These are based on vector averaging [23], relaxation methods [13], and mathematical orientation models [24–26]. The orientation models depend on reliable detection of the core and delta points in the fingerprint image. Most of the methods for singular point extraction [20,18,19] depend on a reliable orientation map (a circular dependency). Therefore, the orientation map has to be estimated to a reasonable accuracy to begin with.

Here we discuss some popular approaches for computing the orientation image. Except in the region of singularities such as core and delta, the ridge orientation varies very slowly across the image. Therefore the orientation image is seldom computed at full-resolution. Instead each non-overlapping block of size $W \times W$ of

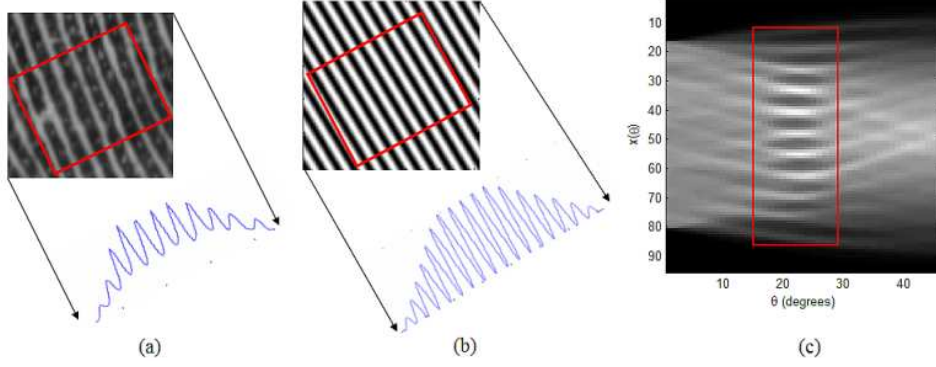


Fig. 5. Projection sum obtained for a window oriented along the ridges (a) Sample fingerprint (b) Synthetic image (c)Radon Transform of the fingerprint region

the image is assigned a single orientation that corresponds to the most probable or *dominant* orientation of the block. The horizontal and vertical gradients $G_x(x, y)$ and $G_y(x, y)$ respectively are computed using simple gradient operators such as a Sobel mask [2]. The block orientation θ is obtained using the following relations

$$G_{yy} = \sum_{u \in W} \sum_{v \in W} 2G_x(u, v)G_y(u, v) \quad (9)$$

$$G_{xx} = \sum_{u \in W} \sum_{v \in W} G_x^2(u, v) - G_y^2(u, v) \quad (10)$$

$$\theta = \frac{1}{2} \tan^{-1} \frac{G_{yy}}{G_{xx}} \quad (11)$$

A rigorous derivation of the above relation is provided in [23]. The dominant orientation so obtained still contains inconsistencies caused by creases and ridge breaks. Utilizing the regularity property of the fingerprint, the orientation image is smoothened. However, due to the ambiguity between 0° and 180° orientations, simple averaging cannot be utilized. Instead the orientation image is smoothened by vector averaging. Each block orientation is replaced with its neighborhood average according to

$$\theta'(i, j) = \frac{1}{2} \tan^{-1} \left\{ \frac{G(x, y) * \sin(2\theta(i, j))}{G(x, y) * \cos(2\theta(x, y))} \right\} \quad (12)$$

Here $G(x, y)$ represents a smoothening kernel such as a Gaussian [2].

2.3.2 Ridge Frequency Image

The ridge frequency map is another intrinsic property of the fingerprint image. The ridge frequency is also a slowly varying property and hence is computed only once for each non-overlapping block of the image. It is estimated based on the projec-

tion sum taken along a line oriented orthogonal to the ridges [3], or based on the variation of gray levels in a window oriented orthogonal to the ridge flow [27]. The projection sum forms a sinusoidal signal and the distance between any two peaks provides the inter-ridge distance. The process of taking the projection is equivalent to computing the Radon transform at the angle of the ridge orientation. As figure 5 shows, the sinusoidal nature of the projection sum is easily visible. More details may be obtained from [3]. Maio and Maltoni [28] proposed a technique that can be used to compute the ridge spacing without performing peak detection. The frequency image so obtained may be further filtered to remove the outliers. However, all these methods depend upon computing a reliable orientation map.

3 Proposed Approach

We present a new fingerprint image enhancement algorithm based on contextual filtering in the Fourier domain. The proposed algorithm is able to simultaneously yield the local ridge orientation and ridge frequency information using short time Fourier Analysis. The algorithm is also able to successfully segment the fingerprint images. The following are some of the advantages of the proposed approach

- (1) The proposed approach obviates the need for multiple algorithms to compute the intrinsic images and replaces it with a single unified approach.
- (2) This is also a more formal approach for analysing the non-stationary fingerprint image than the local/windowed processing found in literature.
- (3) The algorithm simultaneously computes the orientation image, frequency image and the region mask as a result of the short time Fourier analysis. In most of the existing algorithms the frequency image and the region mask depend critically on the accuracy of the orientation estimation.
- (4) The estimate is probabilistic and does not suffer from outliers unlike most maximal response approaches found in literature.
- (5) The algorithm utilized complete contextual information including instantaneous frequency, orientation and even orientation coherence/reliability.

3.1 Overview

Figure 6 illustrates the overview of the proposed approach. During STFT analysis, the image is divided into overlapping windows. It is assumed that the image is stationary within this small window and can be modeled approximately as a surface wave. The fourier spectrum of this small region is analyzed and probabilistic estimates of the ridge frequency and ridge orientation are obtained. The STFT analysis also yields an energy map that may be used as a region mask to distinguish between the fingerprint and the background regions. The orientation image is then used to

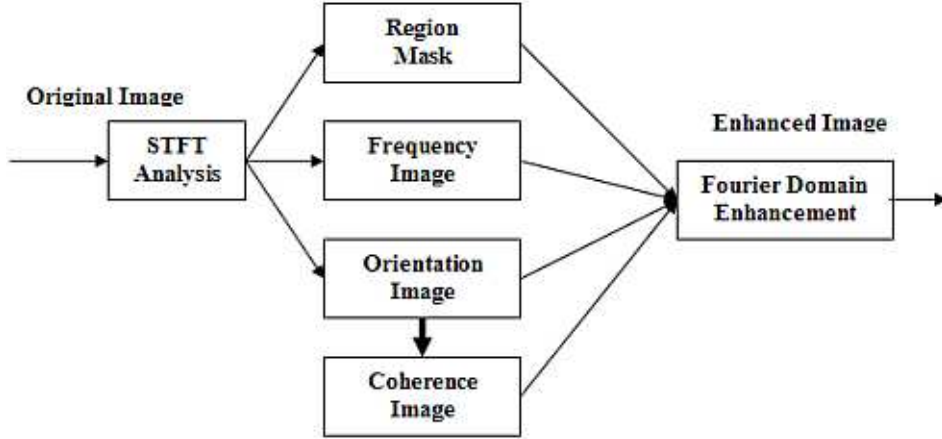


Fig. 6. Overview of the proposed approach

compute the angular coherence [14]. The coherence image is used to adapt the angular bandwidth. The resulting contextual information is used to filter each window in the fourier domain. The enhanced image is obtained by tiling the result of each analysis window.

3.2 Short Time Fourier Analysis

The fingerprint image may be thought of as a system of oriented texture with non-stationary properties. Therefore traditional Fourier analysis is not adequate to analyze the image completely. We need to resolve the properties of the image both in space and also in frequency. We can extend the traditional one dimensional time-frequency analysis to two dimensional image signals to perform short (time/space)-frequency analysis. In this section we recapitulate some of the principles of 1D STFT analysis and show how it is extended to two dimensions for the sake of analyzing the fingerprint.

When analyzing a non-stationary 1D signal $x(t)$ it is assumed that it is approximately stationary in the span of a temporal window $w(t)$ with finite support. The STFT of $x(t)$ is now represented by time frequency *atoms* $X(\tau, \omega)$ [29] and is given by,

$$X(\tau, \omega) = \int_{-\infty}^{\infty} x(t)W^*(t - \tau)e^{-j\omega t}dt \quad (13)$$

In the case of 2D signals such as a fingerprint image, the space-frequency *atoms* is

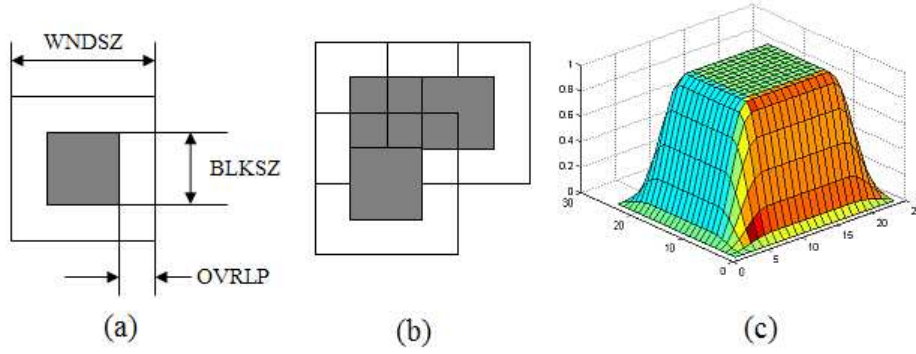


Fig. 7. (a)Overlapping window parameters used in the STFT analysis (b) Illustration of how analysis windows are moved during analysis (c)Spectral window used during STFT analysis

given by,

$$X(\tau_1, \tau_2, \omega_1, \omega_2) = \int_{-\infty}^{\infty} \int_{-\infty}^{\infty} I(x, y) W^*(x - \tau_1, y - \tau_2) e^{-j(\omega_1 x + \omega_2 y)} dx dy \quad (14)$$

Here τ_1, τ_2 represent the spatial position of the two dimensional window $W(x, y)$. ω_1, ω_2 represents the spatial frequency parameters. Figure 7 illustrates how the spectral window is parameterized. At each position of the window, it overlaps OVRLP pixels with the previous position. This preserves the ridge continuity and eliminates 'block' effects common with other block processing image operations. Each such analysis frame yields a single value of the dominant orientation and frequency in the region centered around (τ_1, τ_2) . However, unlike regular Fourier transform, the result of the STFT is dependent on the choice of the window $w(t)$. For the sake of analysis any smooth spectral window such as Hanning, Hamming or even a Gaussian [30] window may be utilized. However, since we are also interested in enhancing and reconstructing the fingerprint image directly from the Fourier domain, our choice of window is fairly restricted. In order to provide suitable reconstruction during enhancement, we utilize a raised cosine window that tapers smoothly near the border and is unity at the center of the window.

With the exception of the singularities such as core and delta any local region in the fingerprint image has a consistent orientation and frequency. Therefore, the local region can be modeled as a surface wave that is characterized completely by its orientation θ and frequency f . It is these parameters that we hope to infer by performing STFT analysis. This approximation model does not account for the presence of local discontinuities but is useful enough for our purpose. A local region of the image can be modeled as a surface wave according to

$$I(x, y) = A \{ \cos(2\pi f(x \cos(\theta) + y \sin(\theta))) \} \quad (15)$$

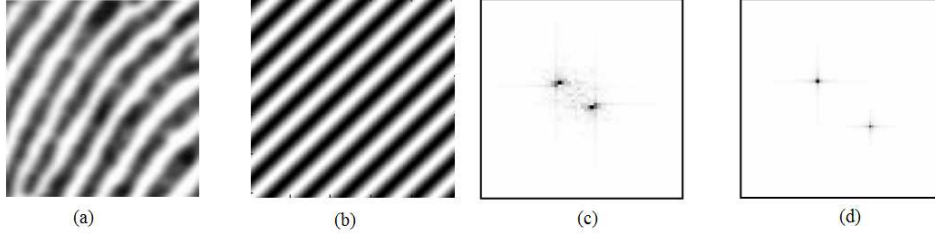


Fig. 8. (a) Local region in a fingerprint image (b) Surface wave approximation (c,d) Fourier spectrum of the real fingerprint and the surface wave. The symmetric nature of the Fourier spectrum arrives from the properties of the Fourier transform for real signals [2]

The parameters of the surface wave (f, θ) may be easily obtained from its Fourier spectrum that consists of two impulses whose distance from the origin indicates the frequency and its angular location indicates the orientation of the wave. However, this straight forward approach is not very useful since the maximum response is prone to errors. Creases running across the fingerprint can easily put off such maximal response estimators. Instead, we propose a probabilistic approximation of the dominant ridge orientation and frequency. It is to be noted that the surface wave model is only an approximation, and the Fourier spectrum of the real fingerprint images is characterized by a distribution of energies across all frequencies and orientations. We can represent the Fourier spectrum in polar form as $F(r, \theta)$. We can define a probability density function $p(r, \theta)$ and the marginal density functions $p(\theta)$, $p(r)$ as

$$p(r, \theta) = \frac{|F(r, \theta)|^2}{\int_r \int_\theta |F(r, \theta)|^2} \quad (16)$$

$$p(r) = \int_\theta p(r, \theta) d\theta \quad (17)$$

$$p(\theta) = \int_r p(r, \theta) dr \quad (18)$$

This interpretation also offers another view of the Fourier spectrum. The spectrum may now thought of to be a distribution of surface waves, with the likelihood of each surface wave being proportional to $|F(r, \theta)|$.

3.3 Ridge Orientation Image

We assume that the orientation θ is a random variable that has the probability density function $p(\theta)$. The expected value of the orientation may then be obtained by performing a vector averaging according to (19). The terms $\sin(2\theta)$ and $\cos(2\theta)$ are

used to resolve the orientation ambiguity between orientations $\pm 180^\circ$.

$$E\{\theta\} = \frac{1}{2} \tan^{-1} \left\{ \frac{\int_{\theta} p(\theta) \sin(2\theta) d\theta}{\int_{\theta} p(\theta) \cos(2\theta) d\theta} \right\} \quad (19)$$

The estimate is also optimal from a statistical sense as shown in [31]. However, if there is a crease in the fingerprints that spans several analysis frames, the orientation estimation will still be wrong. The estimate will also be inaccurate when the frame consists entirely of unrecoverable regions with poor ridge structure or poor ridge contrast. In such instances, we can estimate the ridge orientation by considering the orientation of its immediate neighborhood. The resulting orientation image $O(x,y)$ is further smoothed using vectorial averaging. The smoothed image $O'(x,y)$ is obtained using

$$O'(x,y) = \frac{1}{2} \left\{ \tan^{-1} \frac{\sin(2O(x,y)) * W(x,y)}{\cos(2O(x,y)) * W(x,y)} \right\} \quad (20)$$

Here $W(x,y)$ represent a Gaussian smoothing kernel. It has been our experience that a smoothing kernel of size 3x3 applied repeatedly provides a better smoothing result than using a larger kernel of size 5x5 or 7x7.

3.4 Ridge Frequency Image

The average ridge frequency is estimated in a manner similar to the ridge orientation. We can assume the ridge frequency to be a random variable with the probability density function $p(r)$ as in (17). The expected value of the ridge frequency is given by

$$E\{r\} = \int_r p(r)rdr \quad (21)$$

The frequency map so obtained is smoothed by process of isotropic diffusion. Simple smoothing cannot be applied since the ridge frequency is not defined in the background regions. Furthermore the ridge frequency estimation obtained at the boundaries of the fingerprint foreground and the image background is inaccurate in practice. The errors in this region will propagate as a result of the plain smoothing. The smoothed is obtained by the following.

$$F'(x,y) = \frac{\sum_{u=x-1}^{x+1} \sum_{v=y-1}^{y+1} F(u,v)W(u,v)I(u,v)}{\sum_{v=y-1}^{y+1} W(u,v)I(u,v)} \quad (22)$$

This is similar to the approach proposed in [3]. Here $W(x,y)$ represents a Gaussian smoothing kernel of size 3×3 . The indicator variable $I(x,y)$ ensures that only valid ridge frequencies are considered during the smoothing process. $I(x,y)$ is non zero only if the ridge frequency is within the valid range. It has been observed that the inter-ridge distance varies in the range of 3-25 pixels per ridge [3]. Regions where inter-ridge separation/frequency are estimated to be outside this range are assumed to be invalid.

3.5 Region Mask

The fingerprint image may be easily segmented based on the observation that the surface wave model does not hold in regions where ridges do not exist. In the areas of background and noisy regions, there is very little structure and hence very little energy content in the Fourier spectrum. We define an energy image $E(x,y)$, where each value indicates the energy content of the corresponding block. The fingerprint region may be differentiated from the background by thresholding the energy image. We take the logarithm values of the energy to the large dynamic range to a linear scale.

$$E(x, y) = \log \left\{ \int_r \int_\theta |F(r, \theta)|^2 \right\} \quad (23)$$

The region mask is obtained by thresholding . We use Otsu's optimal thresholding [32] technique to automatically determine the threshold. The resulting binary image is processed further to retain the largest connected component and binary morphological processing [33].

3.5.1 Coherence Image

Block processing approaches are associated with spurious artifacts caused by discontinuities in the ridge flow at the block boundaries. This is especially problematic in regions of high curvature close to the core and deltas that have more than one dominant direction. These problems are clearly illustrated in [4]. To offset this problem, Sherlock and Monroe [13] used a piece wise linear dependence between the angular bandwidth and the distance from the singular point location. However, this requires a reasonable estimation of the singular point location. Most algorithms for singular point location are obtained from the orientation [18,19] map that is noisy in poor quality images (a circular dependency as outlined before). Instead we rely on the flow-orientation/angular coherence measure [14] that is more robust than singular point detection. The coherence is related to dispersion measure of

circular data.

$$C(x_0, y_0) = \frac{\sum_{(i,j) \in W} |\cos(\theta(x_0, y_0) - \theta(x_i, y_i))|}{W \times W} \quad (24)$$

The coherence is high when the orientation of the central block $\theta(x_0, y_0)$ is similar to each of its neighbors $\theta(x_i, y_i)$. In a fingerprint image, the coherence is expected to be low close to the points of the singularity. In our enhancement scheme, we utilize this coherence measure to adapt the angular bandwidth of the directional filter.

3.6 Enhancement

The algorithm for enhancement can now be outlined as follows The algorithm con-

```

Algorithm: FFTEnhance
Inputs   : Image I(x,y)
Outputs  : Enhanced Image I'(x,y), Ridge Orientation Image O(x,y),
          Ridge Frequency Image F(x,y), Energy Image E(x,y),
          Orientation Coherence Image C(x,y), Region Mask(x,y)
STAGE I: STFT Analysis
1. For each overlapping block B(x,y) in the image
   a. Remove DC content of B, B=B-avg(B)
   b. Multiply by spectral window W
   c. Obtain the FFT of the block, F = FFT(B)
   d. Perform root filtering on F
   e. Perform STFT Analysis. The analysis yields values of
      E(x,y), O(x,y), F(x,y)
   end for
2. Smoothen orientation map O(x,y) by vector averaging to yield O'(x,y)
3. Perform isotropic diffusion on frequency map F(x,y) to yield F'(x,y)
4. Compute coherence image C(x,y) using O'(x,y)
5. Compute region mask R(x,y) by thresholding E(x,y)
STAGE II: Enhancement
6. For each overlapping block B(x,y) in the image
   a. Compute angular filter FA centered around O(x,y) and with
      bandwidth inversely proportional to C(x,y)
   b. Compute radial filter FR centered around frequency F(x,y).
   c. Filter the block in the FFT domain, F= F*FR*FA
   d. Compute the enhanced block B'(x,y) = IFFT(F)
   end for
7. Reconstruct the enhanced image by composing enhanced blocks B'(x,y)

```

Fig. 9. Outline of the enhancement algorithm

sists of two stages. The first stage consists of STFT analysis and the second stages performs the contextual filtering. The STFT stage yields the ridge orientation image, ridge frequency image and the block energy image which is then used to compute the region mask. Therefore the analysis phase simultaneously yields all the intrinsic images that are needed to perform full contextual filtering. The filter itself is separable in angular and frequency domains and is identical to the filters men-

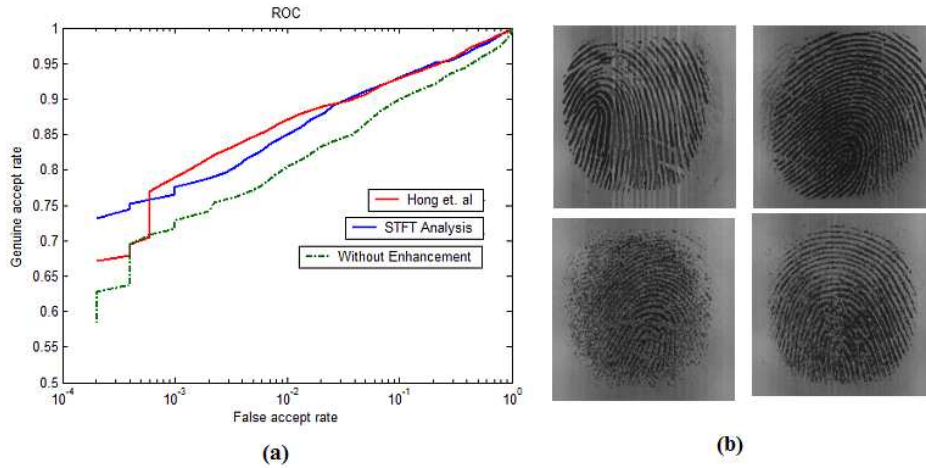


Fig. 10. (a)ROC curves with and without enhancement (FVC2002 DB3 database). It can be seen that the proposed algorithm compares favorably with Gabor based filtering approach, especially in the low false accept region of operation (b) Some examples of adversarial images present in DB3

tioned in [13] and outlined in equations (4). In our algorithm, the radial bandwidth is also adapted for each block to cover two octaves around the central frequency ρ_0 .

4 Experimental Evaluation

The results of each stage of the STFT analysis and the enhancement is shown in Figure 11. It can be seen that the quality of reconstruction is not affected even around the points of high curvature marked by the presence of the singularities. The result of enhancement on several images from FVC database [34] database is shown in Figure 12 and 13. It can be seen that the enhancement improves the ridge structure even in the areas of high ridge curvature without introducing any artifacts. Figure 14 shows the comparative results for a poor quality fingerprint image. While the effect of the enhancement algorithm may be gauged visually, the final objective of the enhancement process is to increase the accuracy of the recognition system. We evaluate the effect of our enhancement on a set of 800 images (100 users, 8 images each) derived from FVC2002 [34] DB3 database. The total number of genuine and impostor comparison are 2800 and 4950 respectively. We used NIST’s NFIS2 open source software (<http://fingerprint.nist.gov>) for the sake of feature extraction and matching. The ROC curves before and after enhancement are as shown in the Figure 4. The summary of the results is provided in Table 1. (These results are improved versions of our work in [35]). The matlab code for the proposed enhancement scheme, Watson’s root filtering approach [15] and Hong et. al’s gabor filtering approach [3] are available from <http://www.eng.buffalo.edu/ssc5>.

Database	Metric	Without Enhancement	Hong et al.	Proposed
DB3	EER	10.35%	7.8%	7.8%
	FMR100	19.50%	13.0%	15.0%

Table 1

Summary of the performance results over FVC2002 DB3. It can be seen that the proposed algorithm compares favorably with Gabor based filtering approach

5 Summary

The performance of a fingerprint feature extraction and matching algorithms depend heavily upon the quality of the input fingerprint image. We presented a new fingerprint image enhancement algorithm based on STFT analysis and contextual/non-stationary filtering in the Fourier domain. The algorithm has several advantages over the techniques proposed in literature such as (i) All the intrinsic images(ridge orientation,ridge frequency, region mask) are estimated simultaneously from STFT analysis. The estimation is probabilistic and is therefore more robust.(ii)The enhancement utilizes the full contextual information(orientation,frequency,angular coherence) for enhancement. (iii) The algorithm has reduced space requirements compared to more popular Fourier domain based filtering techniques. We perform an objective evaluation of the enhancement algorithm by considering the improvement in matching accuracy for poor quality prints. We show that it results in 24.6% relative improvement in recognition rate over a set of 800 images in FVC2002 DB3 [34] database. Our future work includes developing a more robust orientation smoothening algorithm prior to enhancement.

6 Acknowledgements

The authors wish to thank the reviewers for their valuable comments and suggestions.

References

- [1] D. Maio, D. Maltoni, A. K. Jain, S. Prabhakar, Handbook of Fingerprint Recognition, Springer Verlag, 2003.
- [2] Gonzalez, Woods, Eddins, Digital Image Processing, Prentice Hall, 2004.
- [3] L. Hong, Y. Wang, A. K. Jain, Fingerprint image enhancement: Algorithm and performance evaluation, Transactions on PAMI 21 (4) (1998) 777–789.
- [4] S. Greenberg, M. Aladjem, D. Kogan, I. Dimitrov, Fingerprint image enhancement using filtering techniques, in: International Conference on Pattern Recognition, Vol. 3, 2000, pp. 326–329.
- [5] L. O’Gormann, J.V.Nickerson, An approach to fingerprint filter design, Pattern Recognition 22 (1) (1989) 29–38.
- [6] G. Z. Yang, P. Burger, D. N. Firmin, S. R. Underwood, Structure adaptive anisotropic image filtering, Image and Vision Computing 14 (1996) 135–145.
- [7] S. Qian, D. Chen, Joint time-frequency analysis, methods and applications, Prentice Hall, 1996.
- [8] J. Daugman, Complete discrete 2D gabor transform by neural networks for image analysis and compression, Transactions on Acoustics, Speech and Signal Processing 36 (1988) 1169–1179.
- [9] T. S. Lee, Image representation using 2D gabor wavelets, Transactions on PAMI 18 (10) (1996) 959–971.
- [10] A. Sherstinsky, R. W. Picard, Restoration and enhancement of fingerprint images using m-lattice (1994).
- [11] S. T. Acton, D. P. Mukherjee, J. P. Havlicek, A. C. Bovik, Oriented texture completion by am-fm reaction diffusion, IEEE Transactions on Image Processing 10 (6).
- [12] C.-Y. Wen, C.-C. Yu, Fingerprint enhancement using am-fm reaction diffusion systems, Journal of Forensic Science 48 (5).
- [13] B.G.Sherlock, D.M.Monro, K.Millard, Fingerprint enhancement by directional fourier filtering, in: Visual Image Signal Processing, Vol. 141, 1994, pp. 87–94.
- [14] A. R. Rao, A Taxonomy of Texture Descriptions, Springer Verlag.
- [15] C. I. Watson, G. T. Candela, P. J. Grother, Comparison of fft fingerprint filtering methods for neural network classification, NISTIR 5493.
- [16] A. K. Jain, Fundamentals of digital image processing, Prentice Hall International, 1989.
- [17] J. Connell, N. K. Ratha, R. M. Bolle, Fingerprint image enhancement using weak models, in: IEEE International Conference on Image Processing, 2002.

- [18] V. S. Srinivasan, N. N. Murthy, Detection of singular points in fingerprint images, *Pattern Recognition* 25 (2) (1992) 139–153.
- [19] A. M. Bazen, S. Gerez, Extraction of singular points from directional fields of fingerprints, in: *Mobile Communications in Perspective, Annual CTIT Workshop, The Netherlands, 2001*.
- [20] Kawagoe, Tojo, Fingerprint pattern classification, *Pattern Recognition* 17 (3) (1987) 295–303.
- [21] B. M. Mehtre, N. N. Murthy, S. Kapoor, B. Chatterjee, Segmentation of fingerprint images using the directional image, *Pattern Recognition* 20 (1987) 429–425.
- [22] L. Hong, A. K. Jain, S. Pankanti, R. Bolle, Fingerprint enhancement, in: *IEEE WACV, 1996*, pp. 202–207.
- [23] M. Kaas, A. Witkin, Analyzing oriented patterns, *Computer Vision Graphics Image Processing* 37 (4) (1987) 362–385.
- [24] B.G.Sherlock, D.M.Monro, A model for interpreting fingerprint topology, *Pattern Recognition* 26 (7) (1993) 1047–1055.
- [25] Viscaya, Gerhardt, A nonlinear orientation model for global description of fingerprints, *Pattern Recognition* 29 (7) (1996) 1221–1231.
- [26] J. Gu, J. Zhou, A novel model for orientation field of fingerprints, in: *IEEE Computer Society Conference On Computer Vision and Pattern Recognition, 2003*.
- [27] D. Maio, D. Maltoni, Neural network based minutiae filtering in fingerprint images, in: *14th International Conference on Pattern Recognition, 1998*, pp. 1654–1658.
- [28] D. Maio, D. Maltoni, Direct gray scale minutia detection in fingerprints, *Transactions on PAMI* 19 (1).
- [29] S. Haykin, B. V. Veen, *Signals and Systems*, John Wiley and Sons, 1999.
- [30] Rabiner, Schafer, *Digital Processing of Speech Signals*, Prentice Hall International, 1978.
- [31] Papoulis, Pillai, *Probability, Random Variables and Stochastic processes*, Mc Graw Hill, 2002, 4th edition.
- [32] N. Otsu, A threshold selection method from gray level histograms, *IEEE Transactions on Systems, Man and Cybernetics* 9 (1979) 62–66.
- [33] Sonka, Hlavac, Boyle, *Image Processing, Analysis and Machine Vision*, second edition, Thomson Asia, 2004.
- [34] Fingerprint verification competition, <http://bias.csr.unibo.it/fvc2002/>.
- [35] S. Chikkerur, V. Govindaraju, Fingerprint image enhancement using STFT analysis, in: *International Workshop on Pattern Recognition for Crime Prevention, Security and Surveillance (ICAPR 05), 2005*, pp. 20–29.

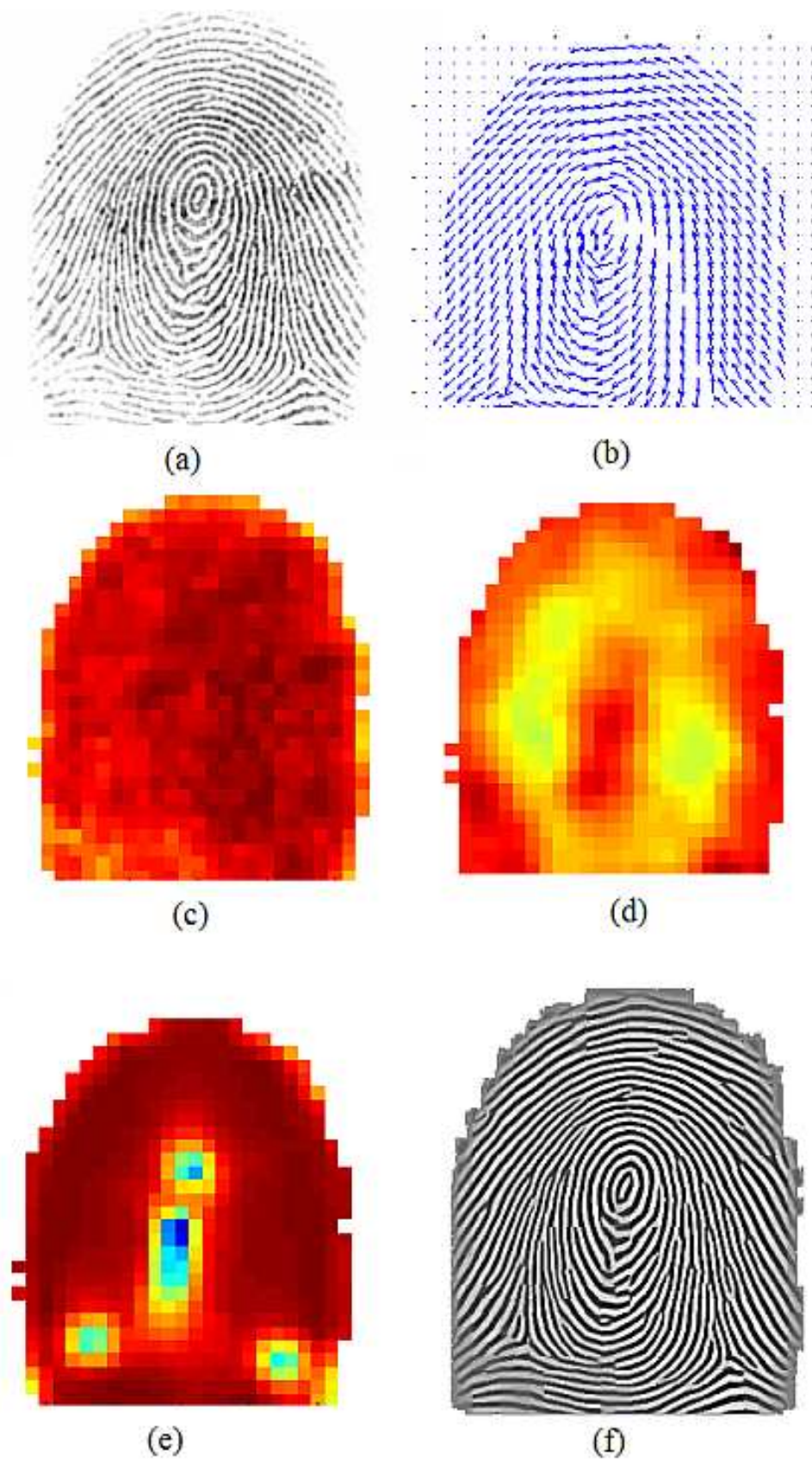


Fig. 11. (a)Original Image (b)Orientation Image (c)Energy Image (d)Ridge Frequency Image (e)Angular Coherence Image (f)Enhanced Image

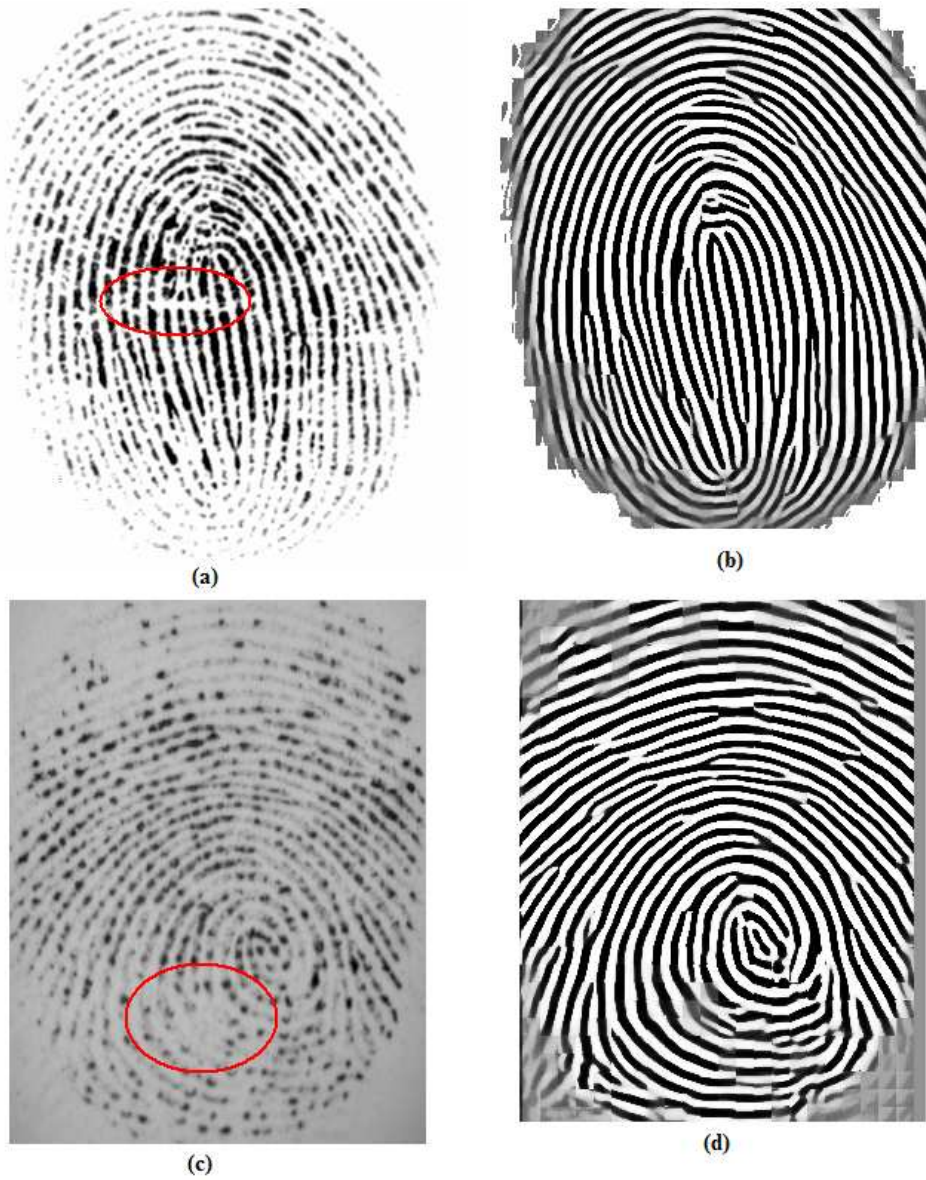


Fig. 12. (a,b)Original and enhanced image(sample taken from FVC2002 DB1 database)
(c,d)Original and enhanced image(sample taken from FVC2002 DB2 database)



(a)



(b)



(c)



(d)

Fig. 13. (a,b)Original and enhanced image(sample taken from FVC2002 DB3 database)
(c,d)Original and enhanced image(sample taken from FVC2002 DB4database)

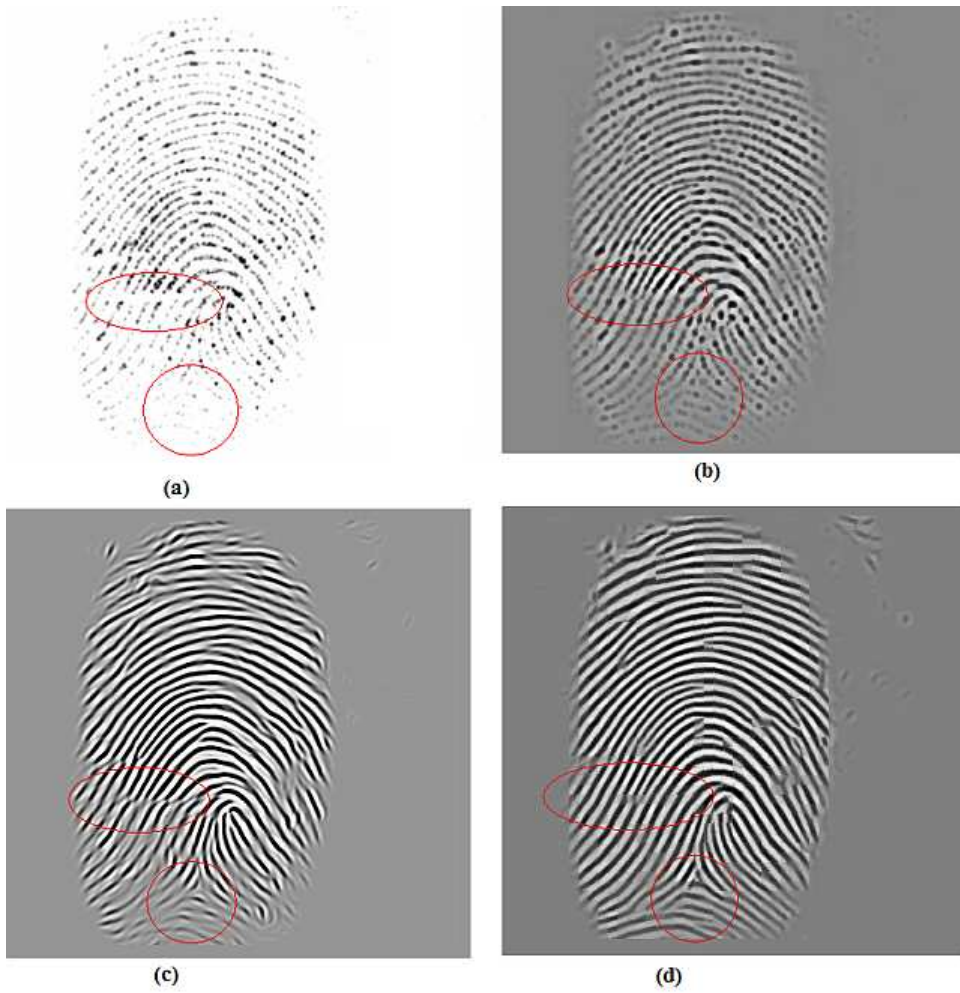


Fig. 14. (a)Original image displaying poor contrast and ridge structure (b)Result of root filtering [15]. (c)Result of Gabor filter based enhancement (d) Result using proposed algorithm